Chapter 12

Ampicillin-Loaded Chitosan Nanoparticles for In Vitro Antimicrobial Screening on *Escherichia coli*

Marilyn Porras-Gómez, Jose Vega-Baudrit and Santiago Núñez-Corrales

Additional information is available at the end of the chapter

http://dx.doi.org/10.5772/intechopen.76034

Abstract

Purpose: To develop ampicillin-loaded chitosan nanoparticles by modified ionic gelation method for evaluating their antimicrobial activity onto *Escherichia coli*.

Methods: Ampicillin-loaded chitosan nanoparticles (CHT-NPs) prepared by ionic gelation method with sodium tripolyphosphate as cross-linking agent. Drug release parameters (zeta potential, particle size, entrapment efficiency, and *in vitro* drug release) were assessed in relation to CHT-NP antimicrobial profile on *E. coli*. Antibacterial properties of CHT-NP formulation with ampicillin were found better than mere ampicillin without CHT-NPs.

Results: SEM, AFM images revealed dimensions of CHT-NPs with irregularity in shape/size. Optimized concentrations of chitosan 0.5% w/v with three different ratios (0.05% to 0.3% w/v) of TPP proved optimal for the evaluation of antibacterial profile of CHT-NPs. *In vitro* ampicillin-loaded CHT-NP delivery studies revealed an initial burst followed by slow sustained drug release, demonstrating superior antimicrobial activity than plain ampicillin, due to the synergistic effect of chitosan and ampicillin.

Conclusion: Chitosan content and cross-linking agent concentrations are control factors in synthesis of the optimized CHT-NP formulation. CHT-NPs with ampicillin cargo capably sustained ampicillin delivery due to NP size and increased surface charge, resulting in efficient growth inhibition in assays with *E. coli*.

Keywords: ampicillin, chitosan nanoparticles, drug delivery, *Escherichia coli*, ionic gelation

1. Introduction

Drug delivery systems are effective for implementing sustained release of many kinds of drugs. Chitosan (CHT), in particular chitosan nanoparticles (CHT-NPs), have been frequently used in drug delivery applications [1]. CHT is the generic name for a family of strongly polycationic derivatives of poly-N-acetyl-D-glucosamine (chitin) found in the exoskeletons of crustaceans such as crabs and shrimps. It can also be found in the cell wall of fungi and bacteria. Structurally, it is a linear polymer of cationic character formed by units of 2-amino-2-deoxy-D-glucose and 2-acetamido-2-deoxy-D-glucose linked by 1–4 bonds [2]. Having a positive charge, CHT is ideal for many drug delivery applications [3, 4]. CHT is biodegradable, non-toxic, non-immunogenic and biocompatible as well as the only naturally occurring polycationic polymer. Along with its derivatives, CHT has received a great deal of attention from the pharmaceutical industry as antimicrobial and antifungal agent [3, 4]. An extensive review of biocompatibility, hydrophilicity, biodegradability and broad spectrum gram-negative/positive antibacterial and anti-fungal effects of chitosan can be found [2].

CHT-NPs exhibit great drug encapsulation efficiency (*EE*) and diverse release profiles, adequate for transporting different types of drugs in many environments [5]. By controlling synthesis parameters conveniently (i.e. reagent concentrations, stirring speed), their diameter, surface charge and other properties can be easily modified thereby leading to a versatile delivery vehicle. CHT-NPs can be synthesized using the ion gelation method with tripolyphosphate (TPP) as cross-linking agent [6, 7]. Ionic cross-linking of CHT is a typical non-covalent interaction, which can be realized by association with negatively charged multivalent ions of TPP. There is a considerable body of literature on the production of CHT-TPP using this method, with many variations concerning the concentrations and ratios of the initial components, of which [1, 7] are seminal works in these matter. Ion gelation allows encapsulation of various compounds, including β-lactams.

Ampicillin is a beta-lactam antibiotic with amino-penicillin skeleton that easily penetrates outer membrane gram-positive/negative bacteria and irreversibly inhibits the transpeptidase enzyme—needed for synthesis of the bacterial cell wall [8]—in the third and final stage of synthesis in binary fission leading cell lysis (bacteriolytic) [9]. Bacterial resistance to antibiotics, including ampicillin, has been observed and investigated for three decades as a serious threat and health crisis [10]. Several mechanisms have been found liking transpeptidase synthesis and activation pathways to bacterial resistance to ampicillin in *E. coli*. Given that ampicillin drug acts as a broad-spectrum penicillin/antibiotic in treatment of infections caused by gram-positive/negative bacteria, and the broad-spectrum β-lactamases among *Enterobacteriaceae* [11] that is evolutionary conserved, finding novel synergistic ways to curb such general and versatile resistance mechanisms is essential for ensuring continued effectiveness of antimicrobial agents [12].

In this work, ampicillin-loaded CHT-NPs were synthesized and the effectiveness of their antimicrobial activity was evaluated against ampicillin and CHT-NPs on *E. coli*. A set of synthesis conditions was investigated in terms of their effect upon particle size, morphology and

surface charge. After selection of the most viable delivery system from the later analysis, the β-lactamic antibiotic (ampicillin) was encapsulated in order to evaluate the encapsulation efficiency of the CHT-NPs. A release profile was obtained in order to assess their applicability as antimicrobial agents against gram-negative bacteria. The aim of the present study is the development of a simple method of synthesis of nano-carriers capable of transporting and releasing a drug such as ampicillin, ultimately inhibiting growth on *E. coli*.

2. Materials and methods

2.1. Reagents

CHT with molecular weight between 100,000 and 300,000 (ACROS Organics™), sodium tripolyphosphate and glacial acetic acid were used. Ultra-pure water was obtained using the Milli-Q A10 system (Millipore). Ampicillin sodium salt (Fisher BioReagents) was used as the antimicrobial agent.

2.2. Bacterial strain

E. coli ATCC 25922 was used for this study.

2.3. Synthesis of chitosan nanoparticles

CHT-NPs were produced using a modified ion gelation method. Briefly, CHT was dissolved at 0.5% w/v in 2% v/v acid acetic solution. Sodium tripolyphosphate was dissolved in ultra-pure water to obtain a 0.1% w/v concentration. An ampicillin volume of 1 ml was then added and later 1 ml of the TPP solution was added drop-wise to 1.5 ml of the CHT solution and magnetically stirred for 1 h. The final suspension was centrifuged at 11,000 rpm for 20 min [6, 13]. Three concentrations of CHT (0.1, 0.3 and 0.5% w/v) and five concentrations of TPP (0.005, 0.01, 0.05, 0.1 and 0.3% w/v) were employed in order to determine their optimal ratio in terms of particle size and surface charge.

2.4. Statistical analysis

In order to evaluate the role of synthesis parameters on particle size and surface charge, including random variations in CHT and then TPP concentrations, selection of linear mixed effects models was performed using standard the Akaike information criterion (AIC), the Bayes information criterion (BIC) and the negative 2 log likelihood criterion (−2LL) [14]. The generalized form (Ω_0^2) of the usual coefficient of determination (R_2) was used [15]. A total of five models (including interactions) were evaluated for each response variable, that is, particle size and ζ potential. Calculations were performed using the *R* Statistical Computing package [16] with the lmer4 package for linear mixed effects models [17]. The Staterthwaite approximation of *p* values was computed for the corresponding observable (**Table 1**) [18].

Model	Response variable	Fixed effects
1	Size	1
2	Size	CHT concentration
3	Size	TPP concentration
4	Size	CHT + TPP concentrations
5	Size	CHT + TPP + CHT*TPP concentrations
6	ζ potential	1
7	ζ potential	CHT concentration
8	ζ potential	TPP concentration
9	ζ potential	CHT + TPP concentrations
10	ζ potential	CHT + TPP + CHT*TPP concentrations

The value of 1 in effects represents the case of a purely random model used as the baseline.

Table 1. Statistical models for evaluating formulations.

2.5. Determination of particle size and ζ potential

The determination of particle size (apparent hydrodynamic diameter) was performed by dynamic light scattering (DLS) and surface electric charge using a Zetasizer Malvern Nano SZ-90 particle analyser, reported as either ζ potential or electrophoretic mobility [7].

2.6. Morphology analysis of CHT-NPs

In order to study the morphology of nanoparticles, topographic images of CHT-NPs were taken on a multi- mode atomic force microscope (AFM) Asylum Research MFP-3D. The AFM probes used for this study were rectangular silicon probes with a nominal spring constant of 40 nN/nm. Similarly, image visualization was carried out in a scanning electron microscope (SEM) Hitachi S-3700 with a 15 nm gold coating on the diluted samples (1/10) using an aluminum base at an acceleration voltage of 15 kV [7].

2.7. Determination of encapsulation efficiency of loaded CHT-NPs

The encapsulation efficiency (*EE*) of the CHT-NPs was determined according to the method described in the previous studies [19]. In brief, the nanoparticle suspensions were separated by centrifuging at 11,000 rpm for 20 min and the contents of ampicillin in the supernatants were measured by HPLC-DAD Perkim Elmer. A blank sample of CHT-NPs without ampicillin was obtained but treated similarly as the drug-loaded CHT-NPs. All samples were measured in triplicate. The *EE* were calculated using.

$$EE = \frac{F}{T} \times 100\% \quad (1)$$

where F is the free amount of ampicillin in the supernatant, T is total amount of ampicillin.

2.8. Release profile of loaded CHT-NP

Release studies were carried out in PBS (pH 7.4) as follows: 1.5 ml ampicillin-loaded CHT-NPs and 1.5 ml PBS were incubated at 37°C and shaken at 200 rpm. Triplicate samples were analyzed at each time step, between 0 and 24 h. The samples were centrifuged and the concentrations of ampicillin released in the supernatant were determined by HPLC-DAD.

2.9. Determination of antimicrobial activity of loaded CHT-NPs

The spectrophotometrically adjusted inoculum (100 μl) of 10^4 bacterial cells was added to each well in the sterile flat-bottomed microtiter plate containing the test CHT-NPs. The design of experiments includes duplicated wells of ampicillin-loaded nanoparticles with three different concentrations of ampicillin (5, 10, 20 mg/ml), two wells with ampicillin as growth inhibition control, two wells containing bacterial suspension with CHT-NPs (growth control) and two wells containing only media (background control) were included in this plate. For the case of wells with ampicillin and CHT-NPs, dilutions were halved at each consecutive level in the gradient. Optical densities were measured for 24 h at 37°C using a multi-detection microplate reader Biotek Synergy HT at 600 nm and automatically recorded for each well every 30 min. Turbidimetric growth curves were obtained depending on the changes in the optical density of bacterial growth for each CHT NP sample and the drug-free growth control.

3. Results and discussion

3.1. Particle size and surface charge of loaded CHT-NPs

Figure 1 corresponds to measures of nanoparticle size (a) and ζ potential (b) according to the concentrations indicated above for both CHT and TPP. As TPP concentration increases, diameter decreases at 0.3 and 0.5% w/v CHT concentrations (a). The opposite occurs at a CHT concentration of 0.1% w/v. In the case of ζ potential (b), all CHT concentrations yield decreasing values as TPP concentration increases.

Statistical models revealed that the best alternative for explaining nanoparticle size in terms of CHT and TPP concentrations is model 5, which includes both factors as well as their interaction (**Table 2**). Both AIC and −2LL have a larger distance from the baseline than in model 3 (size only depending on TPP concentration), being also more significant and with a better fit than it. **Figure 1(a)** shows that nanoparticle size decreases as TPP concentration increases and, simultaneously, CHT concentration decreases. In that sense, model 5 also indicates that while TPP is the largest driver of nanoparticles diameter ($\chi^2 = 3.536$, $df = 4$, $p(\chi^2) < 0.001$), the interaction between CHT and TPP is responsible for the observed change in slope (dotted lines for each line). CHT concentration seems not to have a large role by itself.

A similar analysis was carried out for ζ potential (**Figure 1(b)**). By the same criteria, model 10 was the best criteria for all AIC, BIC and −2LL simultaneously. While all factors are statistically significant, TPP concentration.

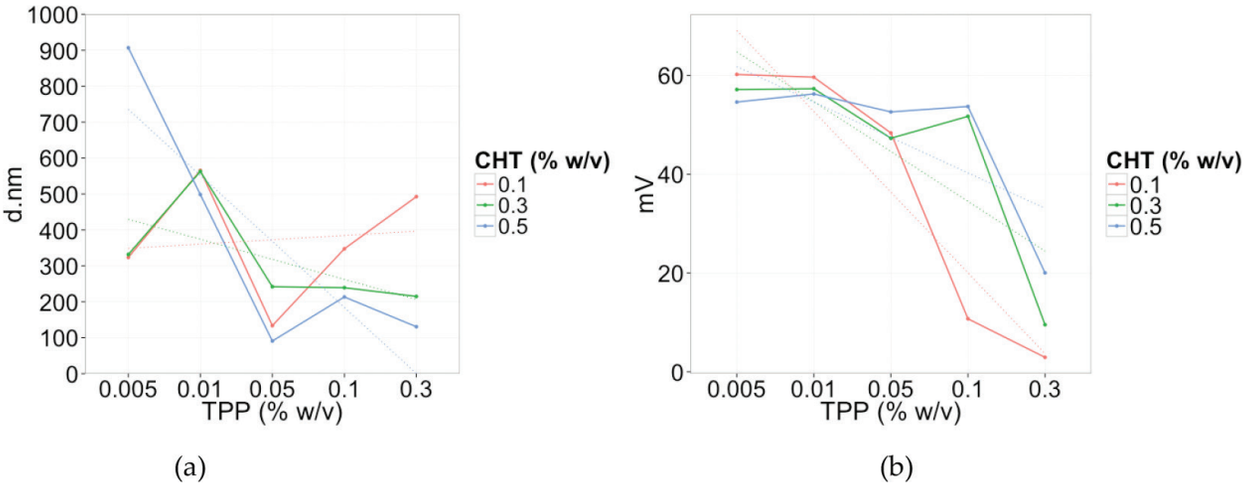

Figure 1. Nanoparticle diameter (nm) and ζ potential (mV) at different concentrations of CHT and TPP. CHT concentration has a marked inverse effect to that of TPP on nanoparticle size, evidence of interference between both factors. A similar trend is identifiable for ζ potential between the lowest and highest TPP concentrations. (**a**) Nanoparticle diameter. (**b**) ζ potential.

Model	*df*	AIC	BIC	−2LL	χ^2	*df* (χ^2)	$p(\chi^2)$	Ω_0^2
2	6	597.35	608.19	−292.67	0.206	2	0.902	0.853
3	8	590.54	604.99	−287.27	10.805	2	0.005*	0.844
4	10	594.11	612.17	−287.05	0.433	2	0.805	0.843
5	18	566.67	599.19	−265.33	43.440	8	<0.001*	0.852

Model 1 is not included (comparison baseline). *Significant *p* values.

Table 2. Results for selection of linear mixed effects models using maximum likelihood for nanoparticles size as the response variable.

central ($\chi^2 = 6604.98$, $df = 4$, $p(\chi^2) < 0.001$): as it increases, ζ potential decreases thanks to a lower amount of available binding sites in the CHT matrix (**Table 3**).

Finally, the most significant levels for both size (diameter in nm) and ζ potential that include CHT and TPP concentrations were identified ($p < 0.001$) as candidates (**Table 4**). In agreement with existing literature, nanoparticles with a large ζ potential ($\zeta \geq 40$ mV) are desirable due to their good stability [20, 21] having sizes in between 200 and 580 nm [5, 22] for the particular case of CHT-NPs. From **Figure 2**, it is clear that levels 1 and 2 reported in **Table 4** (matching Samples M and N in **Table 5**) comply with these requirements. The choice of sample N maximizes the value for the ζ potential while preserving a small nanoparticle size within the range mentioned above.

3.2. Morphology analysis of loaded CHT-NPs

A batch of CHT-NPs without cargo was synthesized and visualized using AFM imaging according to sample preparation N (**Figure 3**). Scan areas are (A) 5 μm × 5 μm and (B) 1 μm × 1 μm respectively for 3A and 3B. The distribution of nanoparticle diameters is reported in **Figure 4** after post-processing of the AFM image.

Model	*df*	AIC	BIC	−2LL	χ^2	*df* (χ^2)	$p(\chi^2)$	Ω_0^2
7	6	278.95	289.79	−133.477	0.862	2	0.650	0.995
8	8	261.73	276.18	−122.866	21.222	2	<0.001*	0.995
9	10	261.64	279.71	−120.822	4.087	2	0.13	0.995
10	18	196.41	228.93	−80.204	81.2370	8	<0.001*	0.995

Model 6 is not included (comparison baseline). *Significant *p* values.

Table 3. Results for selection of linear mixed effects models using maximum likelihood for ζ potential as the response variable.

Level	Concentrations
1	CHT 0.5%w/v, TPP 0.05%w/v
2	CHT 0.5%w/v, TPP 0.1%w/v
3	CHT 0.5%w/v, TPP 0.3%w/v

Only levels with $p < 0.001$ are shown here.

Table 4. Significant levels for CHT and TPP concentrations simultaneously reported in model 5 for nanoparticle size and model 10 for ζ potential.

Additionally, SEM images were performed upon samples with and without ampicillin cargo (**Figure 5**). Images 5A, 5B and 5C are from a CHT-NPs sample. It verifies that CHT-NPs have a dispersed, corrugated and spherical morphology with a diameter between 100 and 200 nm. Complementary, images 5D, 5E and 5F belong to 10 mg/ml ampicillin-loaded CHT-NPs sample with an *EE* more than 40% (**Figure 6**) these samples have a smooth spherical morphology with a diameter between 500 and 1000 nm, showing an aggregation effect between nanoparticles.

3.3. Encapsulation efficiency of loaded CHT-NPs

For encapsulation efficiency (**Figure 6**) the initial ampicillin concentration was compared against final encapsulated concentration (**Figure 6(a)**) and later transformed into *EE* (**Figure 6(b)**). *EE* lies within a range of 15–41% with a peak value at a concentration of ampicillin of 4 mg/ml in the final CHT-NPs solution volume.

3.4. Release profile of loaded CHT-NP

A release profile was obtained for the ampicillin-loaded CHT-NPs (**Figure 7**). Released percentage was calculated in relation to the encapsulated ampicillin concentration. Release percentage oscillates between 5 and 20% across 24 h. The burst effect is clearly observable (between 0 and 2 h), to be later succeeded by a more stable behavior (from 2 to 18 h) and rising finally in the last stage (from 18 to 24 h). The observed pattern suggests that swelling of the first layer in the polymeric matrix releases a large amount of ampicillin in the medium (0–1 h), and becomes more stable until the innermost layers are reached, where the remaining

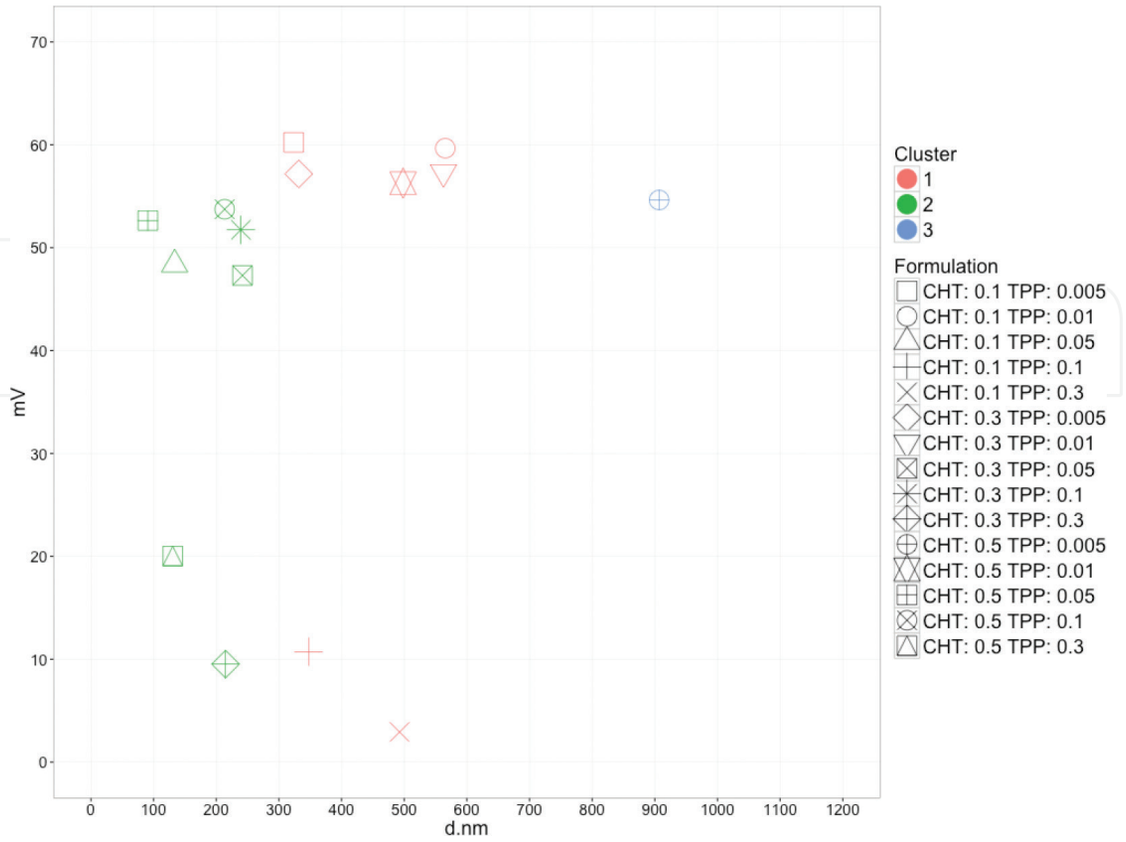

Figure 2. Scatter plot for diameter and surface charge of different CHT-NPs. The classification (clusters) was computed using the Hartigan-Wong *k*-means clustering algorithm [23]. Formulations indicate both CHT and TPP concentrations used for each nanoparticle type. The top left points in the green cluster (above 45 mV and below 300 nm) are the best delivery targets with respect to size and ζ potential, which appear at medium to low concentrations of TPP (0.05–0.1% w/v) and mostly at medium and high concentrations of CHT (except for C with 0.1% w/v). Most experimentally found diameters are below 600 nm. In the case of surface charge, data are partitioned in two groups: above 40 mV and below 20 mV with no nanoparticle in the middle.

Sample	CHT	TPP	*d*	ζ
A	0.1	0.005	323.57 ± 186.84	60.23 ± 2.85
B	0.1	0.01	565.60 ± 97.49	59.67 ± 0.92
C	0.1	0.05	133.60 ± 18.34	48.37 ± 0.31
D	0.1	0.1	347.43 ± 17.60	10.73 ± 0.59
E	0.1	0.3	492.63 ± 16.35	2.92 ± 0.16
F	0.3	0.005	331.73 ± 168.06	57.17 ± 2.28
G	0.3	0.01	562.73 ± 155.08	57.33 ± 2.06
H	0.3	0.05	241.90 ± 34.51	47.30 ± 0.53
I	0.3	0.1	239.30 ± 27.14	51.73 ± 1.25
J	0.3	0.3	214.93 ± 11.40	9.53 ± 0.40
K	0.5	0.005	906.97 ± 264.60	54.63 ± 2.26
L	0.5	0.01	498.30 ± 49.73	56.27 ± 0.95

Sample	CHT	TPP	d	ζ
M	0.5	0.05	90.88 ± 30.90	52.63 ± 2.53
N	0.5	0.1	213.50 ± 29.76	53.73 ± 3.33
O	0.5	0.3	130.56 ± 15.65	20.03 ± 1.46

CHT and TPP concentrations are given in terms of w/v percentage. Diameter d is given in nm. ζ potential is given in mV. Standard deviation is included in both cases.

Table 5. CHT and TPP concentrations for synthesis of nanoparticles in **Figure 2**.

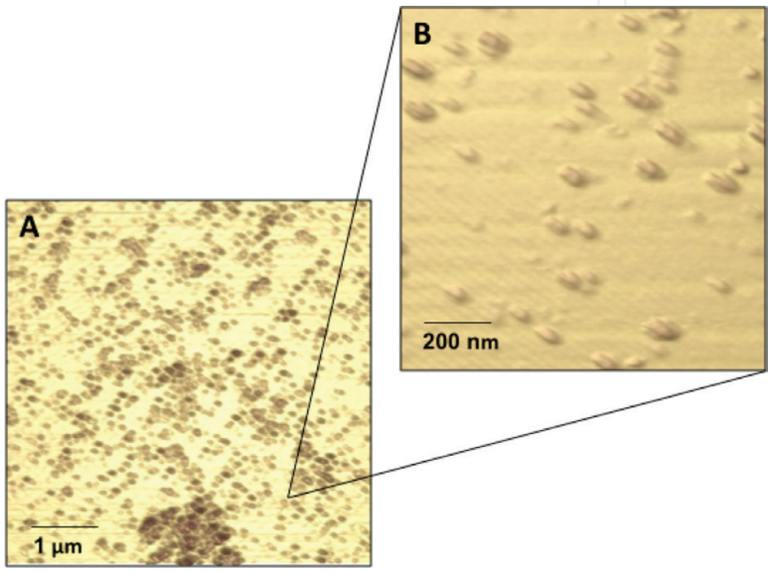

Figure 3. AFM image of CHT-NPs without ampicillin cargo. AFM images were performed as a first assessment of CHT-NP synthesis process. **Figure 5** provides the contrast between these nanoparticles and ampicillin loaded CHT-NPs. **A** corresponds to a scan area of 5 μm × 5 μm and **B** to 1 μm × 1 μm.

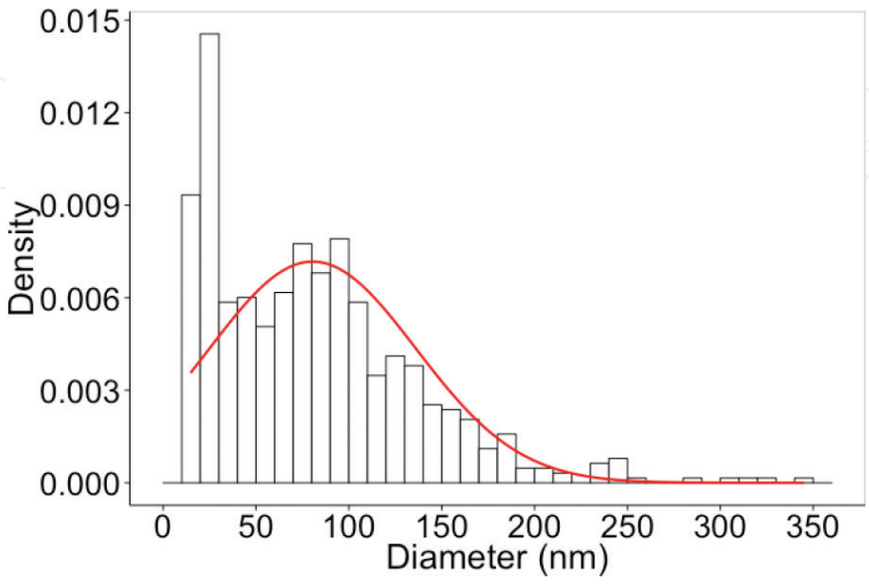

Figure 4. Histogram of CHT-NPs diameters for the AFM image in **Figure 3**. $N = 632$, $\bar{d} = 80.5$ nm, $\sigma_d = 55.6$ nm.

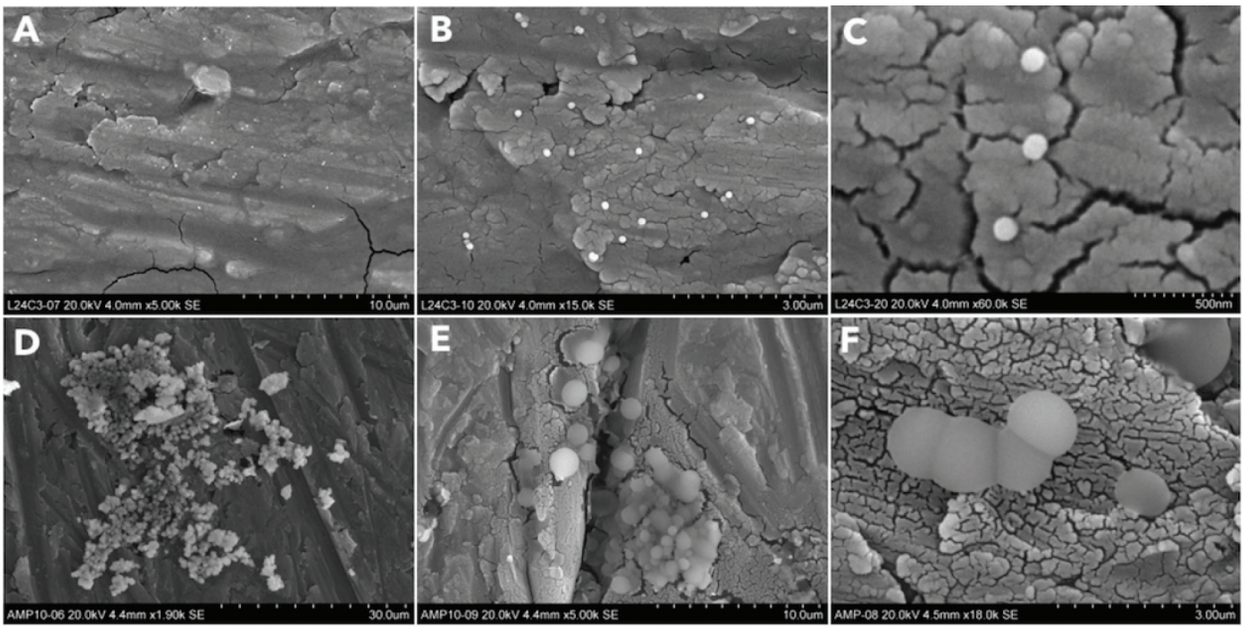

Figure 5. SEM image of CHT-NPs, without and with antibiotic cargo (ampicillin). **A**, **B** and **C** are images of nanoparticles without cargo and **D**, **E** and **F** encapsulate ampicillin. Nanoparticle diameter and size appears to increase in order to gain stability in ampicillin-loaded nanoparticles, which also has an additional aggregation effect.

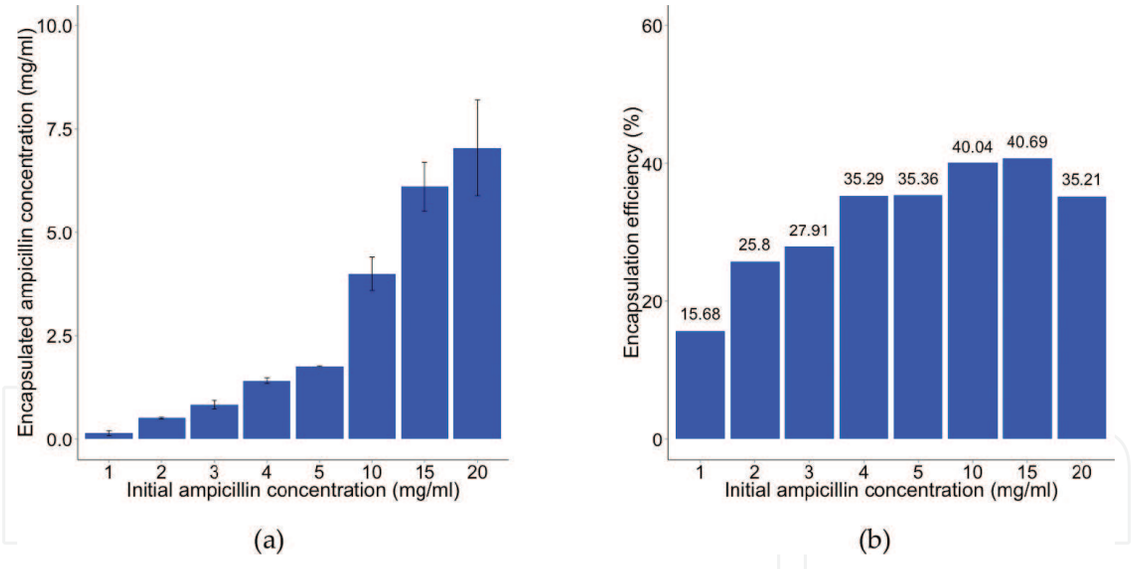

Figure 6. Cargo efficiency of the CHT-NPs from initial concentrations, obtained as described in [19]. (**a**) Measured encapsulated ampicillin concentration through HPLC. (**b**) Corresponding encapsulation efficiency, calculated as *EE* in Eq. (1).

contents are finally released. The latter is consistent with what is described by Carbinato et al. [24] for cross-linked pectin/high-amylose starch matrices.

3.5. Growth inhibition assays for *E. coli* ATCC 25922

Figure 8 shows the growth inhibition assays for *E. coli* ATCC 25922, an ampicillin–susceptible reference strain. Under the conditions of this assay, this strain shows a minimal inhibitory

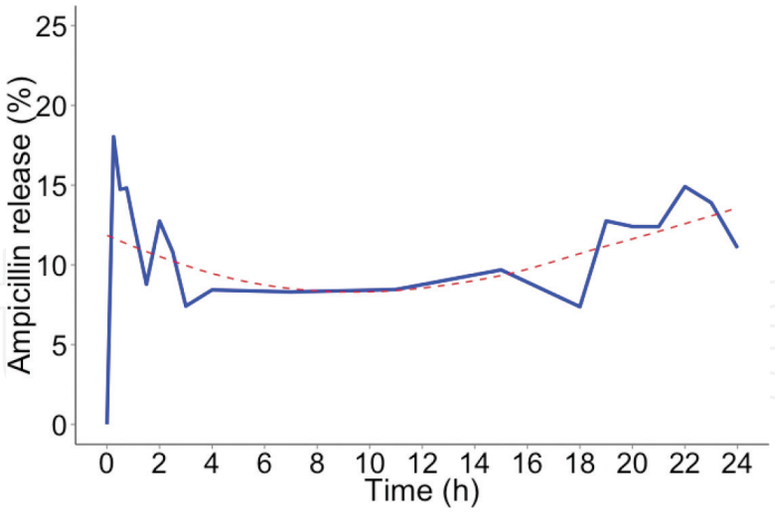

Figure 7. Release profile of ampicillin-loaded CHT-NPs. A burst effect was observed for the first hour, followed by a stabilization phase (1–4 h), a steady release phase (4–15 h) and posterior relative increase (15–24 h).

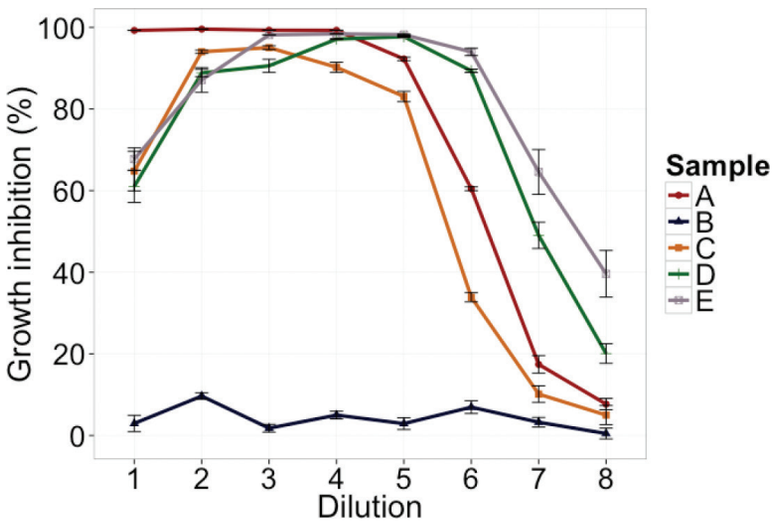

Figure 8. Growth inhibition assays for *E. coli*. Samples are as follows: (**A**) ampicillin 20 mg/ml, (**B**) CHT-NPs, ampicillin-loaded NPs at (**C**) 5 mg/ml, (**D**) 10 mg/ml and (**E**) 20 mg/ml. As expected, sample **B** produces no inhibition, while **A–C** remain effective until the fifth dilution and **D–E** to the sixth dilution.

concentration (MIC) of 2 μg/ml, which is in agreement with the range values (2–8 μg/ml) previously reported [25]. A clinical *E. coli* isolate is considered as non-susceptible when its MIC value is >8 μg/ml. The highest ampicillin concentration used as control was 500 μg/ml (dilution 1, **Figure 8**), generating a concentration gradient by double dilutions through 3.91 μg/ml (dilution 8, **Figure 8**). The three ampicillin-loaded CHT-NPs systems (C, D and E) show a similar growth inhibition pattern with respect to the positive control (ampicillin), indicating that under these conditions ampicillin is released from CHT − NPs to concentrations high enough to inhibit bacterial growth. Moreover, both CHT − NPs systems D and E, loaded with 10 mg/ml and 20 mg/ml of ampicillin respectively, maintain growth inhibition with more dilutions with respect to ampicillin. It is worth noting that inhibition in samples A and C lower their effectiveness rapidly after the fifth dilution, but samples D and E have a much wider range of inhibition at lower concentrations for all remaining dilutions.

4. Conclusions

CHT-NPs synthesis was successfully achieved and the manipulation of CHT and TPP concentrations towards optimization for drug delivery resulted in smaller particles and increased surface charge. Besides, a detailed physicochemical characterization of CHT-NPs was obtained. CHT-NPs were able to encapsulate and release ampicillin. The encapsulation efficiency of ampicillin CHT-NPs exceeds 30% in most cases while antibiotic release maintains a relatively stable profile, ranging between 5 and 20% in a 24-hour period. A microbiological assay was used as proof of principle in order to verify the release of the antibiotic ampicillin from the CHT-NPs systems. Growth inhibition of the ampicillin-susceptible *E. coli* ATCC 25922 reference strain was achieved in a similar pattern compared with ampicillin alone.

In terms of the obtained release profile in a period of 24 h, several comparisons can be drawn in terms of other alternatives. The cumulative release profile, computed from data shown in **Figure 7**, indicates that less than 40% of the cargo was released after 24 h. Ampicillin-loaded electrospun poly(ε-caprolactone) nanofiber yarns have a much faster release profile, releasing more than 90% of its cargo in the same period [26]. By contrast, our formulation has a release profile faster than that reported for ampicillin-conjugated gum Arabic microspheres [27]. In the later cases, no additional antibiotic or bacteriostatic effect is present in the polymeric matrix. CHT-NPs loaded with ampicillin reported here are comparable to chitosan microgranules loaded with diclofenac sodium in contrast to chitosan beads loaded with diclofenac sodium in terms of the order of magnitude of released antibiotic [28]. Compared against ampicillin loaded methylpyrrolidinone chitosan and chitosan microspheres, our nanoparticles have a significantly lower encapsulation efficiency [29], yet the former are not suitable for sustained release. CHT-NPs are similar in size compared to existing literature on ampicillin-loaded nanoparticles and liposomes [30], with a release profile closer to that of liposomes. In the later study, liposomes had a larger inhibition halo at lower dilutions than nanoparticles of higher density and longer release time.

Finally, the synthesis protocol of CHT-NPs elaborated in this study constitutes a platform for the analysis of the encapsulation of other antibiotics with different structures as well as for assays on other bacteria.

Acknowledgements

The authors wish to acknowledge funding and support from the National Center for Advanced Technology Studies (CeNAT) and the National Council of Rectors for the period comprehended between 2012 and 2015.

Conflict of interest

The authors have no conflict of interest to declare.

Author details

Marilyn Porras-Gómez, Jose Vega-Baudrit* and Santiago Núñez-Corrales

*Address all correspondence to: jvegab@gmail.com

National Nanotechnology Laboratory, National Center for Advanced Technology Studies, San José, Costa Rica

References

[1] Liu H, Gao C. Preparation and properties of ionically cross-linked chitosan nanoparticles. Polymers for Advanced Technologies. 2009;**20**(7):613-619

[2] Cota-Arriola O, Cortez-Rocha MO, Burgos-Hernández A, Ezquerra-Brauer JM, Plascencia-Jatomea M. Controlled release matrices and micro/nanoparticles of chitosan with antimicrobial potential: Development of new strategies for microbial control in agriculture. Journal of the Science of Food and Agriculture. 2013;**93**(7):1525-1536

[3] Morris GA, Kök SM, Harding SE, Adams GG. Polysaccharide drug delivery systems based on pectin and chitosan. Biotechnology and Genetic Engineering Reviews. 2010; **27**(1):257-284

[4] Nasti A, Zaki NM, de Leonardis P, Ungphaiboon S, Sansongsak P, Rimoli MG, Tirelli N. Chitosan/tpp and chitosan/tpp–hyaluronic acid nanoparticles: systematic optimisation of the preparative process and preliminary biological evaluation. Pharmaceutical Research. 2009;**26**(8):1918-1930

[5] Gan Q, Wang T. Chitosan nanoparticle as protein delivery carrier—Systematic examination of fabrication conditions for efficient loading and release. Colloids and Surfaces B: Biointerfaces. 2007;**59**(1):24-34

[6] Ajun W, Yan S, Li G, Li H. Preparation of aspirin and probucol in combination loaded chitosan nanoparticles and in vitro release study. Carbohydrate Polymers. 2009; **75**(4):566-574

[7] Fàbregas A, Miñarro M, García-Montoya E, Pérez-Lozano P, Carrillo C, Sarrate R, Sánchez N, Ticó JR, Suñé-Negre JM. Impact of physical parameters on particle size and reaction yield when using the ionic gelation method to obtain cationic polymeric chitosan–tripolyphosphate nanoparticles. International Journal of Pharmaceutics. 2013; **446**(1):199-204

[8] Nguyen-Distèche M, Pollock JJ, Ghuysen J-M, Puig J, Reynolds P, Perkins HR, Coyete J, Salton MRJ. Sensitivity to ampicillin and cephalothin of enzymes involved in wall peptide crosslinking in *Escherichia coli* k12, strain 44. The FEBS Journal. 1974;**41**(3):457-463

[9] Blumberg PM, Strominger JL. Interaction of penicillin with the bacterial cell: penicillin-binding proteins and penicillin-sensitive enzymes. Bacteriological Reviews. 1974; **38**(3):291

[10] Neu HC. The crisis in antibiotic resistance. Science. 1992;**257**(5073):1064-1074

[11] Smet A, Martel A, Persoons D, Dewulf J, Heyndrickx M, Herman L, Haesebrouck F, Butaye P. Broad-spectrum β-lactamases among enterobacteriaceae of animal origin: Molecular aspects, mobility and impact on public health. FEMS Microbiology Reviews. 2010;**34**(3):295-316

[12] Pamela A Hunter, K Coleman, Jackie Fisher, and Dalveen Taylor. In vitro synergistic properties of clavu-lanic acid, with ampicillin, amoxycillin and ticarcillin. Journal of Antimicrobial Chemotherapy. 1980;**6**(4):455-470

[13] Ji J, Hao S, Danjun W, Huang R, Yi X. Preparation, characterization and in vitro release of chitosan nanoparticles loaded with gentamicin and salicylic acid. Carbohydrate Polymers. 2011;**85**(4):803-808

[14] Adams E, Coomans D, Smeyers-Verbeke J, Massart DL. Application of linear mixed effects models to the evaluation of dissolution profiles. International Journal of Pharmaceutics. 2001;**226**(1):107-125

[15] Ronghui X. Measuring explained variation in linear mixed effects models. Statistics in Medicine. 2003;**22**(22):3527-3541

[16] R Core Team. R: A Language and Environment for Statistical Computing. Vienna, Austria: R Foundation for Statistical Computing; 2013. Available from: http://www.R–project.org/

[17] Bates D, Maechler M, Bolker B, Walker S, Christensen RHB, Singmann H. Linear mixed-effects models using Eigen and S4. R package version 1.0-5. 2013

[18] Schaalje GB, McBride JB, Fellingham GW. Adequacy of approximations to distributions of test statistics in complex mixed linear models. Journal of Agricultural, Biological, and Environmental Statistics. 2002;**7**(4):512-524

[19] Sibaja B. Nanopartículas de Quitosano como Sistema de Liberación Controlada de Principios Activos [Master's thesis]. Heredia, Costa Rica: Facultad de Ciencias Extactas y Naturales, Universidad Nacional; 2011

[20] O'Brien RW et al. Electroacoustic studies of moderately concentrated colloidal suspensions. Faraday Discussions of the Chemical Society. 1990;**90**:301-312

[21] Hanaor D, Michelazzi M, Leonelli C, Sorrell CC. The effects of carboxylic acids on the aqueous dispersion and electrophoretic deposition of zro 2. Journal of the European Ceramic Society. 2012;**32**(1):235-244

[22] Gan Q, Wang T, Cochrane C, McCarron P. Modulation of surface charge, particle size and morphological properties of chitosan-tpp nanoparticles intended for gene delivery. Colloids and Surfaces B: Biointerfaces. 2005;**44**(2):65-73

[23] Hartigan JA, Wong MA. Algorithm as 136: A k-means clustering algorithm. Journal of the Royal Statistical Society. Series C (Applied Statistics). 1979;**28**(1):100-108

[24] Carbinato FM, de Castro AD, Evangelista RC, Cury BSF. Insights into the swelling process and drug release mechanisms from cross-linked pectin/high amylose starch matrices. Asian Journal of Pharmaceutical Sciences. 2014;**9**(1):27-34

[25] JB Patel, FR Cockerill, J Alder, PA Bradford, GM Eliopoulos, DJ Hardy, et al. Performance standards for antimicrobial susceptibility testing; twenty-fourth informational supplement. CLSI Standards for Antimicrobial Susceptibility Testing. 2014;**34**(1):1-226

[26] Liu H, Leonas KK, Zhao Y. Antimicrobial properties and release profile of ampicillin from electrospun poly (ε-caprolactone) nanofiber yarns. Journal of Engineered Fibers and Fabrics. 2010;**5**(4):10-19

[27] Nishi KK, Antony M, Jayakrishnan A. Synthesis and evaluation of ampicillin-conjugated gum arabic microspheres for sustained release. Journal of Pharmacy and Pharmacology. 2007;**59**(4):485-493

[28] Gupta KC, Ravi Kumar MNV. Drug release behavior of beads and microgranules of chitosan. Biomaterials. 2000;**21**(11):1115-1119

[29] Giunchedi P, Genta I, Conti B, Muzzarelli RAA, Conte U. Preparation and characterization of ampicillin loaded methylpyrrolidinone chitosan and chitosan microspheres. Biomaterials. 1998;**19**(1):157-161

[30] Fatal E, Rojas J, Roblot-Treupel L, Andremont A, Couvreur P. Ampicillin-loaded liposomes and nanoparticles: Comparison of drug loading, drug release and in vitro antimicrobial activity. Journal of Microencapsulation. 1991;**8**(1):29-36

IntechOpen